energies

Article

Experimental Study on Denitration Transformation of CFB Boiler Burning Fujian Anthracite

Wenting Zhou [1,2], Hongzhou He [1,2,*] and Huanghuang Zhuang [1,2]

1 Key Laboratory of Energy Cleaning Utilization and Development of Fujian Province, Jimei University, Xiamen 361021, China
2 Cleaning Combustion and Energy Utilization Research Center of Fujian Province, Jimei University, Xiamen 361021, China
* Correspondence: hhe99@jmu.edu.cn

Abstract: Two 75 t/h medium-temperature separated circulating fluidized bed boilers burning Fujian anthracite were upgraded with low NOx combustion (LNC). By reducing the effective cross-sectional area of the air distributor (from 13.43 m^2 to 11.38 m^2), improving the secondary air rate (from 40% to 45%), adjusting the secondary air supply method (adding a layer of upper secondary air, raising the height of the lower secondary air nozzle (0.4 m), and increasing the secondary air speed (from 48 m/s to 54 m/s), the reform of low nitrogen combustion was carried out. The transformation achieved remarkable results, i.e., the original NOx emission concentration can be controlled between 140–160 mg/m^3 after the transformation, and the lowest value is below 120 mg/m^3.

Keywords: CFB boiler; denitration transformation; low NOx combustion; Fujian anthracite

Citation: Zhou, W.; He, H.; Zhuang, H. Experimental Study on Denitration Transformation of CFB Boiler Burning Fujian Anthracite. *Energies* **2023**, *16*, 2535. https://doi.org/10.3390/en16062535

Academic Editor: Jaroslaw Krzywanski

Received: 14 February 2023
Revised: 1 March 2023
Accepted: 3 March 2023
Published: 8 March 2023

1. Introduction

As people pay more and more attention to environmental protection, the emission standards for NOx and other air pollutants are becoming increasingly stringent. Circulating Fluidized Bed (CFB) boilers, developed in the 1970s [1–5], have the advantages of higher combustion efficiency, lower pollutant emissions (the NOx emission levels generally range from 150 to 300 mg·m^{-3}), wider fuel adaptability, and larger operating load range and are therefore widely used in many fields [6–9].

At present, the total NOx emission and the maximum allowable emission concentration have clear requirements at home and abroad. "Standards of performance for electric utility steam generating units" [10] issued by the US Environmental Protection Agency (EPA) in 2015 specifies the NOx emission limit of 135 mg/m^3. In 2002, the European Union revised and issued "On the limitations of certain pollutants into the air from large combustion plants, directive 2001/80/EC of the European parliament and of council" [11], which reduced the NOx emission limit of units over 500 MW from 650 mg/m^3 to 200 mg/m^3. According to the "Emission standards for air pollutants from thermal power plants" (GB 13223-2011) implemented on 1 January 2012 [12], it is specified that according to the different combustion modes, location and operational time, coal-fired boilers are required to have NOx (standard, dry base, baseline oxygen content of 6%, the same as below) emission limits of 200 mg/m^3 (W-shaped flame furnace boiler, CFB boiler, etc.) and 100 mg/m^3 (newly built boiler, key areas). The ultra-net emission co-proposed by the National Development and Reform Commission, the Ministry of Environmental Protection, and the National Energy Administration requires that NOx emission concentration should not be higher than 50 mg/m^3 [13]. Fujian Province has demanded that all coal-fired power boilers with transformation conditions have a NOx emission limit of 50 mg·m^{-3} (Minhuanfa [2016] No. 6) [14], and new coal-fired power generation units must achieve ultra-low emission levels. The NOx emission concentration of the current medium-temperature separated CFB boilers burning Fujian anthracite coal can meet the

NOx emission limit of GB 13223-2011 for the existing CFB boilers at 200 mg·m^{-3}; however, they cannot meet the requirements of the NOx emission limit of 50 mg·m^{-3} in Fujian Province, so denitrification transformation is an imperative.

In this paper, the Low NOx Combustion (LNC) technology [15–17] is adopted. Starting from the source of NOx generation, it aims to provide an industrial application reference for the NOx compliance transformation of CFB boilers burning Fujian anthracite coal.

2. Experiment Conditions

The experiment was conducted on a DG75/3.82-11 CFB boiler of China Fujian Shishi Thermoelectric Co., Ltd., which has a depth of 5.905 m, a width of 4.645 m, and a height of 32.34 m, as shown in Figure 1.

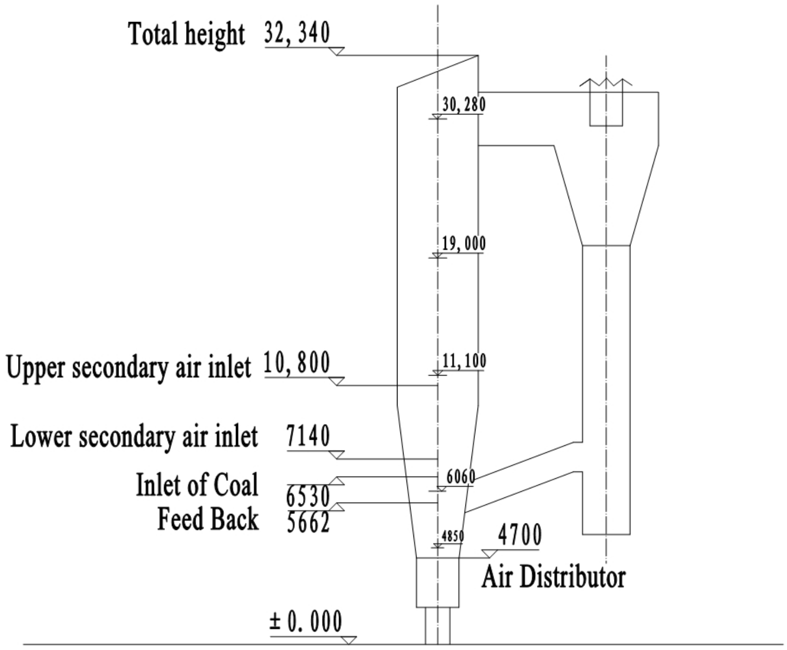

Figure 1. Structural schematic diagram of CFB boiler burning Fujian anthracite. Unit: mm.

The boiler adopted staged combustion technology, in which the combustion air included the primary air, the secondary air, and the coal seeding air. The hot primary air was divided into a left stream and a right one, and entered the dense phase area of the combustion chamber from the isobaric water-cooled air chamber at the bottom of the furnace through the air cowl. The secondary air was divided into a lower layer with the nozzle center elevation of 7.14 m and an upper layer with the nozzle center elevation of 10.80 m, and was injected into the furnace chamber through 32 nozzles arranged on the front and rear walls. The coal seeding air was from the hot primary air and pressurized by the booster fan, and entered the furnace chamber through the coal chute with a center elevation of 6.53 m. The size of the air distributor was 2501 mm × 5905 mm. There were six temperature sensors installed on the chamber, with elevations of 4850 mm, 6060 mm, 11,100 mm, 14,400 mm, 19,000 mm and 30,280 mm, respectively, to measure the temperature distribution in the furnace chamber. An additional temperature sensor was mounted on the rear flue.

The design and operation parameters of the boiler are shown in Table 1. The proximate and ultimate analysis of the experimental coals is shown in Table 2.

Data including temperature, pressure, and air flow were collected on the distributed control system (DCS), and the arithmetic mean values were used. There was a YDZX-01 flue gas monitoring device at the outlet of the dust collector with a precision of 2%; the UV differential spectrometric method was used to measure the composition and concentration of the flue gas emissions.

Table 1. Design and operating parameters of the boiler.

Items	Value	Items	Value
Rated evaporation/($t{\cdot}h^{-1}$)	75	Temperature at 4850 mm/°C	950–980
Superheated steam pressure /(MPa)	3.82	Temperature at 6060 mm/°C	930–990
Superheated steam temperature/°C	450	Temperature at 11,100 mm/°C	900–1000
Feed-water temperature/°C	150	Temperature at 14,400 mm/°C	850–1020
Cold air temperature/°C	20	Temperature at 19,000 mm/°C	850–1050
Exhaust temperature/°C	120–150	Temperature at 30,280 mm/°C	520–580

Table 2. Ultimate analysis and proximate analysis of the experimental coals.

	Proximate Analysis (%)					Ultimate Analysis (%)				
	Mt	**Aar**	**Vdaf**	**FCar**	**Qar.net /(MJ·kg^{-1})**	**Car**	**Har**	**Oar**	**Nar**	**Sar**
Design coal	12.73	15.35	3.69	68.23	22.39	68.86	0.30	1.64	0.22	0.90
Experimental coal (I)	9.0	30.0	3.8	57.2	20.68	57.41	1.16	1.02	0.56	0.85
Experimental coal (II)	8.60	21.93	2.37	67.1	24.27	65.03	0.95	1.50	1.21	0.78

Note: Mt is the total moisture of raw coal sample, %; Aar is the base ash received from coal, %; Vdaf is coal dry ash free volatile matter, %; FCar is coal receipt-based fixed carbon, %; Qar.net is received base low calorific value, MJ/kg; Car is the carbon content of coal received base, %; Har is the hydrogen content of coal received base, %; Oar is coal received base oxygen content, %; Nar is the nitrogen content of coal received base, %; Sar is the sulfur content of coal base, %.

3. LNC Transformation and Results

3.1. Reducing the Effective Cross-Sectional Area of Air Distributor

On the basis of ensuring good fluidization of the bed material, the effective cross-sectional area of air distributor was reduced from 13.43 m^2 to 11.38 m^2, a 15.26% reduction, by increasing the thickness of wear-resistant castable of the water-cooled wall in the dense phase zone. At the same time, the secondary air rate β was increased from 40% to 45%. According to the Chinese standard PCTC (Performance check up test code for flue gas denitrification equipment of coal-fired power plants) [18], experimental coal (I) was selected for the thermal test. During the experiment, the limestone-gypsum wet desulfurization WFGD (wet flue gas desulfurization) system was put into normal operation. In order to make the test results more comparable, the boiler load, coal feed, and other key parameters were kept stable.

3.1.1. Effect of the Excess Air Coefficient on NOx Emission

Figure 2 shows the effect of the excess air coefficient, λ, on NOx emission for the secondary air rate, β, of 45%, and the boiler loads of 75 t/h and 64 t/h.

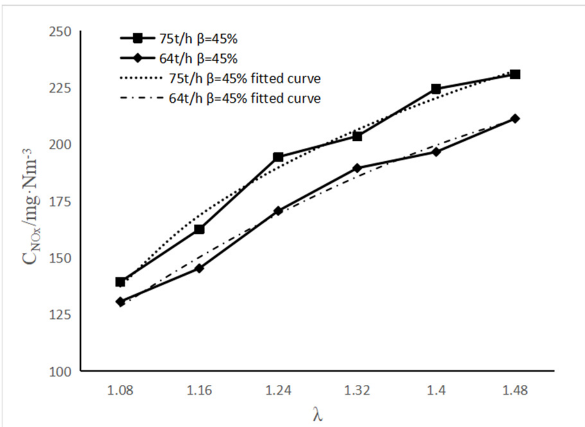

Figure 2. Effect of λ on C_{NOx} in combustion flue gas.

Figure 2 shows that the NOx emission concentration, C_{NOx}, rises significantly in the initial period and then increases much more slowly with the increase of λ. Hence, an open downward parabolic trend is presented in Figure 2. In addition, the NOx emission concentration C_{NOx} at 75 t/h load condition is higher than that of 64 t/h and grows faster.

When λ is increased, the O_2 concentration, CO_2, also increases, which enhances the anthracite combustion intensity, accelerates the NOx generation rate, and increases the NOx emission concentration, C_{NOx}. In addition, the NOx emission concentration, C_{NOx}, also increases with the increasing boiler load and volumetric thermal load of the furnace chamber, which is consistent with the experimental results of the higher C_{NOx} at 75 t/h [19].

3.1.2. Effect of the Secondary Air Rate on NOx Emission Concentration

Figure 3 shows the effect of the secondary air rate, β, on the NOx emission concentration, C_{NOx}, in the combustion flue gas when λ is 1.2, and the boiler loads are 75 t/h and 64 t/h.

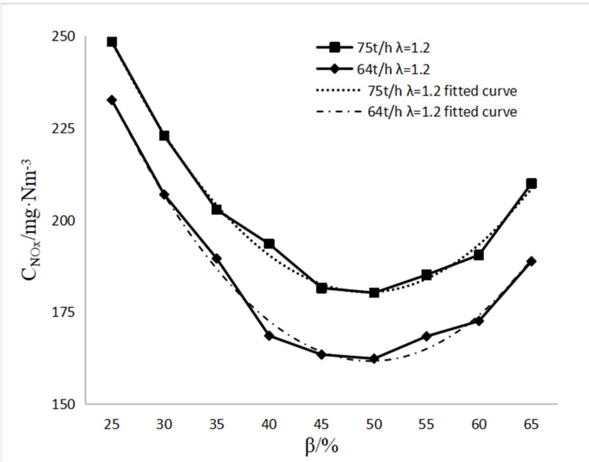

Figure 3. Effect of β on C_{NOx} in the combustion flue gas.

As seen in Figure 3, when β < 35%, the NOx emission concentration, C_{NOx}, decreases rapidly with the increase of β; when β varies in the range of 35% to 55%, C_{NOx} remains basically stable; when β > 55%, C_{NOx} increases slightly with the increase of β. This indicates that when the excess air coefficient, λ, remains constant, there exists an optimal value for the secondary air rate, β, in the range of approximately 40% to 55%, which can lead to the minimum C_{NOx}.

β plays a dual role in the NOx generation. With the increase of β, the primary air rate decreases, the oxygen in the dense phase area is deficient, and the reduction combustion produces a large amount of incomplete combustion products such as NH_3, CO, HCN, H_2, and coke particles, which suppresses the NOx generation. On the contrary, the O_2 concentration above the secondary air area increases, the afterburning intensity of the Fujian anthracite combustion is enhanced, and the NOx emission concentration, C_{NOx}, increases.

3.1.3. Effect of the Upper Secondary Air Rate on NOx Emission Concentration

Figure 4 illustrates the effect of the upper secondary air rate, k_{up}, i.e., the ratio of the upper secondary air flow rate to the total secondary air flow rate, on the NOx emission concentration, C_{NOx}, in the combustion flue gas when λ is 1.2, β is 45%, and the boiler loads are 75 t/h and 64 t/h.

As shown in Figure 4, with the increase of k_{up}, the NO_X concentration in the flue gas changes in an open upward parabolic trend, i.e., C_{NOx} first decreases ($k_{up} \leq 45\%$) and then increases ($k_{up} > 55\%$). There exists an optimal value of the upper secondary air rate, k_{up}, which results in the lowest value of the NO_X emission concentration, C_{NOx}, in the flue gas. As can be seen from Figure 4, this optimum value is between 45% and 55%.

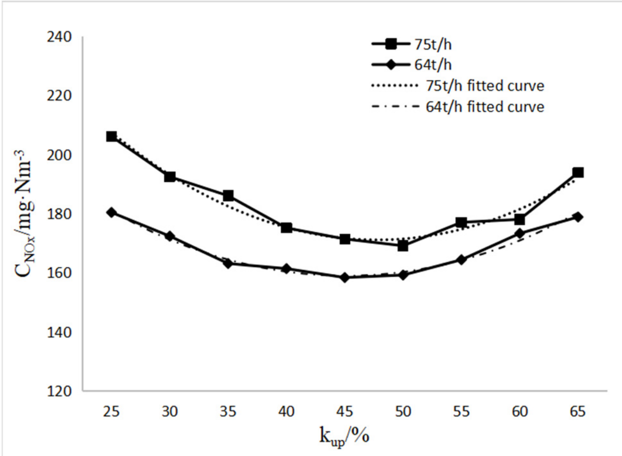

Figure 4. Effect of k_{up} on C_{NOx}.

The upper secondary air rate, k_{up}, plays a dual role in the NOx generation.

On one hand, with the increase of k_{up}, the lower secondary air flow decreases, and the fluidization speed in the area between the upper secondary air and the lower secondary air decreases. Therefore, the residence time of coal particles is prolonged, the reducing atmosphere in the dense phase area is improved, and the generation and emission of NOx are reduced. On the other hand, as k_{up} increases, a large amount of oxygen is supplemented into the furnace chamber through the upper secondary air outlet, which will enhance the combustion intensity of the coal particles, strengthen the afterburning of the Fujian anthracite coal, and increase the flue gas temperature at the furnace exit, which will increase the generation of NOx in the combustion flue gas.

3.1.4. Effect of β and k_{up} on the Mechanical Incomplete Combustion Heat Loss and CO Emission Concentration

Figures 5 and 6 show the effects of the varying secondary air rate, β, and upper secondary air rate, k_{up}, on the boiler mechanical incomplete combustion heat loss, q_4, and CO emission concentration, C_{CO}, when the excess air factor, λ, is 1.2 and the boiler load is 75 t/h.

q4 is incomplete mechanical loss, including incomplete combustion loss of flight machinery and incomplete combustion loss of slag machinery. Fly ash sampling in the test was carried out in the boiler horizontal flue in front of the electrostatic precipitator, and was extracted by the 3012H soot tester developed by Qingdao Laoshan Institute of Applied Technology. Each extraction time was 5 min. The slag was sampled manually at the slag discharge port of the boiler every 1 h, with about 5 kg slag comprising the sample. According to the provisions of GB/T 212-2008 "Method for Industrial Analysis of Coal" and GB/T 176-2017 "Method for Chemical Analysis of cement", the difference between the combustion loss of fly ash (or slag) and its general volatiles (Mad+Vad) is the carbon content of fly ash (or slag) with particle size Cfh (Clz). Thus, the electrostatic precipitator was used to undertake the dry ash under the ash bucket of the tank truck. The quality of the heavy truck and the empty truck was measured by the SCS-50 automobile scale with the precision grade of III, produced by Xuzhou Ramqi Technology Company. The quality difference was the quality of the fly ash. Similarly, the TCS-520F-300 electronic platform scale with 1/3000 precision developed by Shanghai Taiheng Instrument , Shanghai, China. Co., Ltd. was used to measure the quality of slag. In summary, the ash and slag ratio can be calculated. q4 can be calculated by the following formula.

$$q_4 = \frac{32866 * A_{ar}\%}{Q_r}\left(a_{lz} * \frac{C_{lz}}{100 - C_{lz}} + a_{fh} * \frac{C_{fh}}{100 - C_{fh}}\right) \quad (1)$$

From Figures 5 and 6, it can be seen that the CO emission concentration, C_{CO}, decreases sharply with the increase of the secondary wind rate, β, and upper secondary wind rate, k_{up}, and then decreases slowly to a stable value. The mechanical incomplete combustion heat loss, q_4, shows an open upward parabolic with the increase of secondary wind rate, β, and upper secondary wind rate, k_{up}, and there exists an optimal β and k_{up}, making q_4 minimum. As seen in Figures 5 and 6, the values of the optimal β and k_{up} are in the range of 45% to 55%.

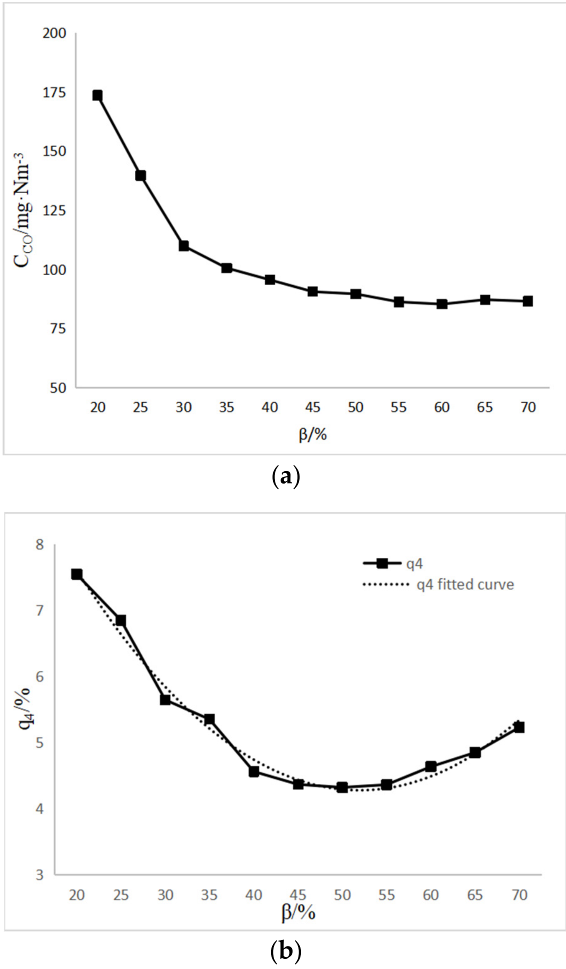

Figure 5. Influence of β on q_4 and CO emission concentration. (**a**) Influence of β on q_4. (**b**) Influence of β on CO emission concentration.

3.2. Secondary Air System Transformation

The transformation scheme was as follows. Firstly, the height of the lower secondary air nozzle was raised by 0.5 m. Then, the middle secondary air was added at 12.65 m elevation of front and rear water-cooled walls. In other words, a layer of secondary air nozzle was added, and a middle second air nozzle was connected with the primary air pipe. (i.e., a pipe was introduced from the hot primary air duct and linked to the master pipe of the upper secondary air duct). The designed air speed of the middle secondary air nozzle was increased from 48 m/s to 54 m/s, and the air box and main duct (Φ600 mm × 5 mm) were lowered from the original elevation of 12.54 m to 12.04 m. The following tests were conducted using experimental coal type (II).

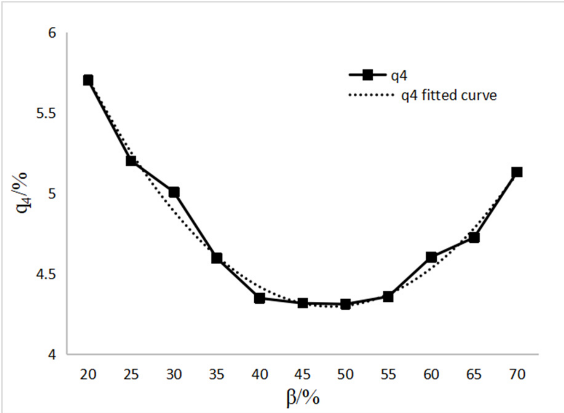

(**a**)

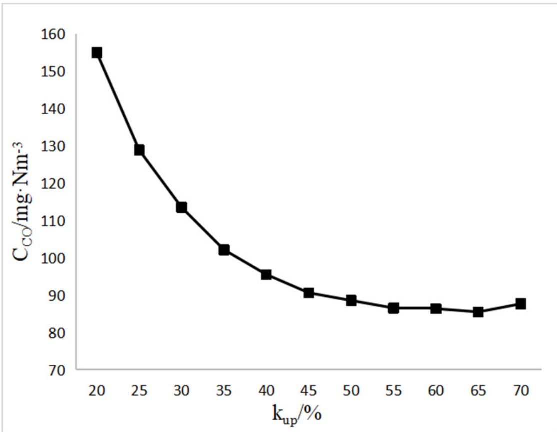

(**b**)

Figure 6. Influence of k_{up} on q_4 and CO emission concentration. (**a**) Influence of k_{up} on q_4. (**b**) Influence of k_{up} on CO emission concentration.

3.2.1. Effect of the Secondary Air Rate on NOx Emission Concentration

Figure 7 shows the effect of the variation the secondary air rate, β, on the NOx emission concentration, C_{NOx}, in the case of keeping the primary air flow, 79 km^3/h, and the upper secondary air flow, 26.3 km^3/h, constant.

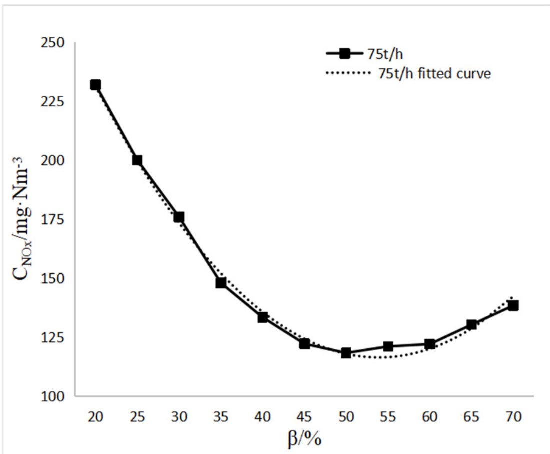

Figure 7. Influence of β on C_{NOx}.

From Figure 7, it can be found that the NOx emission concentration, C_{NOx}, varies with the secondary air rate, β, in an open upward parabolic. Along with the increase of the secondary wind rate β, C_{NOx} shows a rapid decline and then decreases slowly. When β is larger than 55%, C_{NOx} increases with the increase of β. After the denitrification transformation, the optimum value of β was shifted from 40% to 50% (Figure 3) before the retrofit to 50% to 60% (Figure 7). It was shown that the increase of the secondary air rate could effectively inhibit the fuel-based NOx conversion and NOx generation, thus reducing the NOx emission concentration [20].

3.2.2. Effect of the Middle Secondary Air Rate on NOx Emission Concentration

Figure 8 shows the effect of the change in the middle secondary air rate, k_m, on the NOx emission concentration, C_{NOx}, when the air excess factor, λ, is 1.2 and the secondary air rate, β, is 50%, in the case of keeping the primary air flow, 79 km^3/h, and the upper secondary air flow, 26.3 km^3/h, constant.

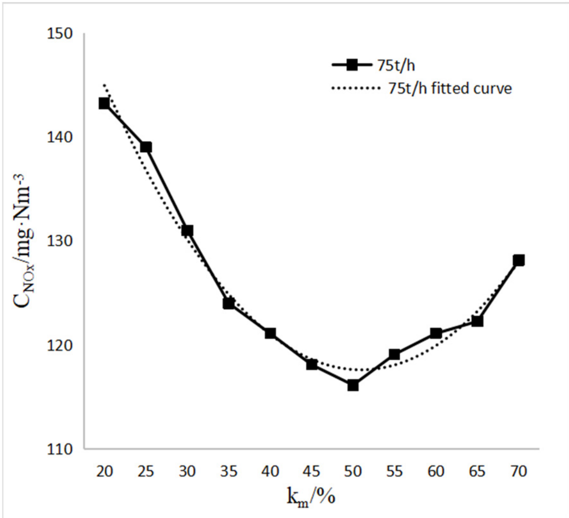

Figure 8. Influence of k_m on C_{NOx}. Notes: $k_m = \dfrac{\text{middle secondary air flow}}{\left(\begin{array}{c}\text{upper secondary air flow} \\ +\text{middle secondary air flow} \\ +\text{lower secondary air flow}\end{array}\right)}$.

.

From Figure 8, it can be seen that NOx emission concentration, C_{NOx}, decreases and then increases with the increase of the middle secondary air rate, k_m, and overall shows an open upward parabolic. The minimum value of C_{NOx} occurs when k_m is between 45% and 55%.

With the increase of k_m, the lower secondary air flow decreases, the fluidization velocity in the area below the middle secondary air becomes smaller, and the reducing atmosphere in this area is enhanced, which prolongs the residence time of coal particles in the reducing atmosphere and reduces the amount of NOx generation and emission.

On the other hand, the O_2 concentration in the furnace chamber increases with the increase of k_m, which enhances the afterburning combustion intensity of the Fujian anthracite [21], raises the smoke temperature at the outlet, increases the combustion of coke N and volatile fraction N in the Fujian anthracite, and adds to the NOx emissions. Therefore, k_m plays a dual role in the NOx emission.

3.2.3. Effect of the Upper Secondary Air Rate on NOx Emission Concentration

Figure 9 shows the effect of the variation of the upper secondary air rate, k_{up}, on the NOx emission concentration, C_{NOx}, in the flue gas, when the air excess coefficient, λ, is 1.2 and the primary air flow, 79 km^3/h, is essentially constant.

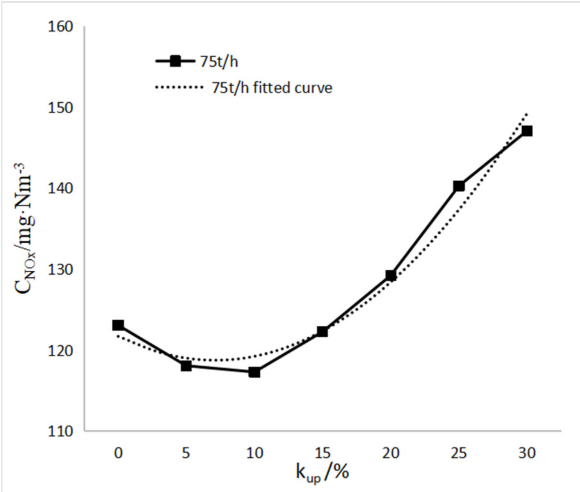

Figure 9. Influence of k_{up} on C_{NOx}.

From Figure 9, with the increase of the upper secondary air rate, k_{up}, the NOx emission concentration, C_{NOx}, in flue gas appears to decrease ($k_{up} \leq 10\%$) and then increase ($k_{up} > 15\%$). With the increase of k_{up}, the penetration range of the upper secondary air increases, the material is stirred and mixed more uniformly, the heat transfer intensity in the center area of the furnace chamber increases, and the effect of graded combustion is obvious, which effectively suppresses the NOx generation. However, when k_{up} is more than 15%, with the continuous increase of k_{up}, the introduction of a large amount of upper secondary air leads to the increase of O_2 concentration, which enhances the afterburning of the Fujian anthracite particles and increases NOx generation in the flue gas.

3.2.4. Effect of the Secondary Air Rate, the Middle Secondary Air Rate, and the Upper Secondary Air Rate on the Mechanical Incomplete Combustion Heat Loss

Figures 10–12 show the effect of β, k_m, and k_{up} on the mechanical incomplete combustion heat loss, q_4, when the air excess factor, λ, is 1.2.

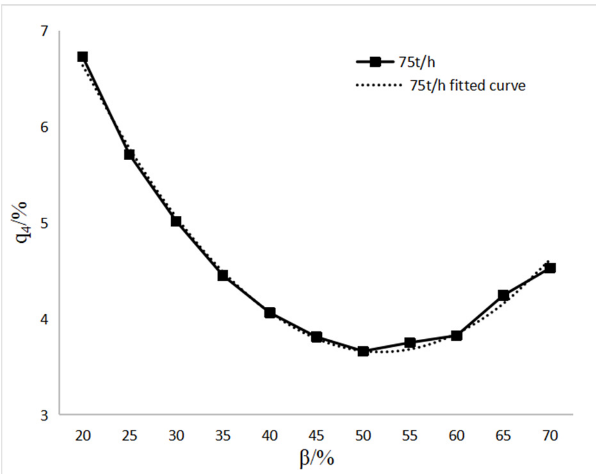

Figure 10. Influence of β on q_4.

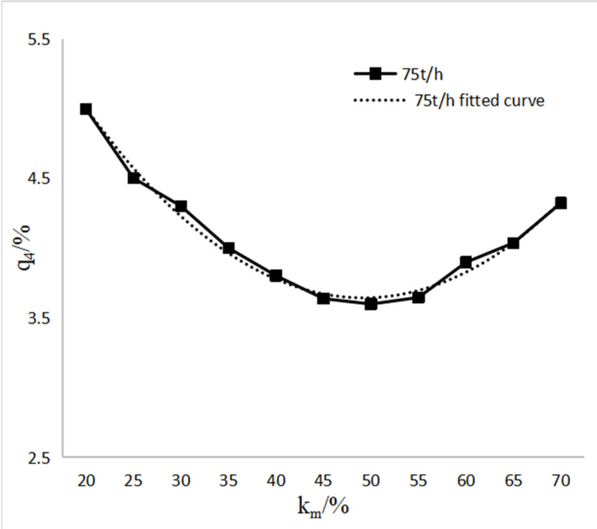

Figure 11. Influence of k_m on q_4.

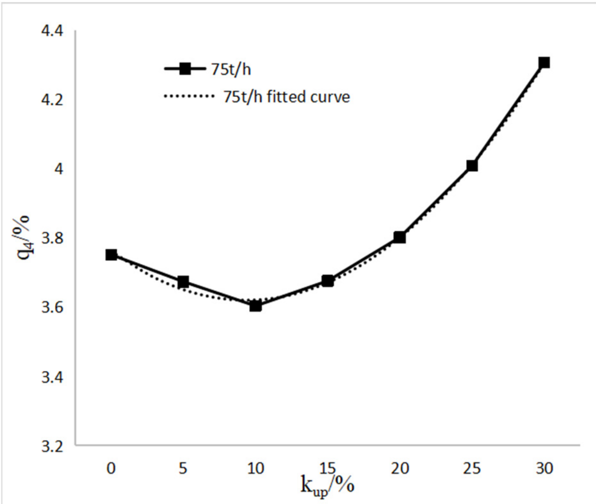

Figure 12. Influence of k_{up} on q_4.

From Figures 10–12, when the λ remains constant, the three curves of q_4 vary with the adjustment of secondary air rate, β, middle secondary air rate, k_m, and upper secondary air rate, k_{up}, and hence all appear as open upward parabolas. Therefore, there must exist an optimal β, k_m, and k_{up} that minimizes the mechanical incomplete combustion heat loss, q_4. From Figures 10 and 11, the optimal values of β and k_m are between 45% and 55%. From Figure 12, the optimal values of k_{up} are between 10% and 15%.

4. Conclusions

In this paper, a denitrification transformation experiment was conducted on a 75/t CFB boiler burning Fujian anthracite using the NOx combustion technology (LNC). The conclusions are summarized as follows.

(1) NOx emission is reduced from about 220 mg/m^3 to about 180 mg/m^3 by reducing the cross-sectional area of the air distributor by 15.26% and increasing the secondary air rate to 45%.

(2) On the basis of reducing the effective cross-sectional area of the air distributor, NOx emission concentration is reduced from about 180 mg/m^3 to about 140 mg/m^3, with the lowest value of the NOx emission concentration below 120 mg/m^3, and the mechanical incomplete combustion heat loss is also reduced by 1.0–1.5%, which

results from adding a layer of the upper secondary air, raising the height of the lower secondary air nozzles by 0.5 m, and increasing the lower and middle secondary air speeds to 54 m/s. The economics of the boiler have been effectively improved.

(3) For a 75 t/h medium temperature cyclone CFB boiler burning Fujian anthracite, the optimum range of the secondary air rate β is 50% to 60% at an excess air factor of 1.2. Under the same circumstances, the optimum middle secondary air rate is 45% to 55%, and the optimum upper secondary air rate is 10% to 15%.

Author Contributions: Conceptualization, W.Z.; methodology, W.Z. and H.H.; software, W.Z.; formal analysis, W.Z.; investigation, H.Z.; re-sources, H.H.; data curation, W.Z.; writing—original draft preparation, W.Z.; writing—review and editing, H.H. and H.Z.; supervision, H.H.; project administration, H.H.; funding acquisition, H.H. All authors have read and agreed to the published version of the manuscript.

Funding: This research received no external funding.

Conflicts of Interest: The authors declare no conflict of interest.

Abbreviations

Symbol	Meaning
CFB	circulating fluidized bed
LNC	low NOx combustion
Mt	total moisture of raw coal sample, %
Aar	base ash received from coal, %
Vdaf	coal dry ash free volatile matter, %
FCar	coal receipt-based fixed carbon, %
Qar.net	received base low calorific value, MJ/kg
Car	carbon content of coal received base, %
Har	hydrogen content of coal received base, %
Oar	coal received base oxygen content, %
Nar	nitrogen content of coal received base, %
Sar	sulfur content of coal base, %
β	secondary air rate, %
λ	excess air coefficient
k_m	middle secondary air rate, %
C_{NOx}	NOx emission concentration, mg/Nm^3
C_{CO}	CO emission concentration, mg/Nm^3
k_{up}	upper secondary air rate, %
q_4	mechanical incomplete combustion heat loss, %
Q_r	heat input per kg of fuel, kJ/kg
C_{lz}	combustible in ash residue of cold ash hopper, %
C_{fh}	combustible in fly ash, %
a_{lz}	mass share of ash content in ash of cold ash hopper in total ash content, %
a_{fh}	mass share of ash content in total ash content of fly ash, %

References

1. Wu, J. *Research & Development for Reducing NOx Emission on Two 75t/h CFB Boiler Burning Fujian Anthracite with Medium-Temperatue Cyclone*; Jimei University: Xiamen, China, 2016. [CrossRef]
2. Liu, Z.; Ma, S.; Pan, X.; Chen, J. Experimental study on the load response rate under the dynamic combined combustion of PC coal and CFB coal in a CFB boiler. *Fuel* **2018**, *236*, 445–451. [CrossRef]
3. Ke, X.; Engblom, M.; Yang, H.; Brink, A.; Lyu, J.; Zhang, M.; Zhao, B. Prediction and minimization of NOx emission in a circulating fluidized bed combustor: A comprehensive mathematical model for CFB combustion. *Fuel* **2021**, *309*, 122133. [CrossRef]
4. Kong, R.; Li, W.; Wang, H.; Ren, Q. Optimization of oxy-fuel circulating fluidized bed combustion system with high oxygen concentration. *Energy Rep.* **2022**, *8*, 83–90. [CrossRef]
5. Chen, H.; Song, Y.; Shi, Y.; Yang, X. Prediction of particle circulation rate in an internally circulating fluidized bed with a central draft tube. *Powder Technol. Int. J. Sci. Technol. Wet Dry Part. Syst.* **2021**, *380*, 497–505. [CrossRef]

6. Huang, Z.; Deng, L.; Che, D. Development and technical progress in large-scale circulating fluidized bed boiler in China. *Front. Energy* **2020**, *14*, 699–714. [CrossRef]
7. Zhang, H.; Gao, M.; Liu, C.; Liu, J.; Yue, G.; Zhang, J. Dynamic prediction of in-situ SO_2 emission and operation optimization of combined desulfurization system of 300 MW CFB boiler. *Fuel* **2022**, *324*, 124421. [CrossRef]
8. Jiang, L.; Li, Y.; Yao, Y.; Zhang, M.; Lu, J.; Huang, Z.; Zhou, T.; Yue, G. Heat transfer and protection of high-temperature reheater of a 660MW circulating fluidized bed boiler after black out. *Appl. Therm. Eng.* **2022**, *213*, 118654. [CrossRef]
9. Jiang, M.; Xiao, P. *Large-Scale Circulating Fluidized Bed Combustion Technologies*; China Power Press: Beijing, China, 2009; pp. 171–175.
10. US EPA. *Standards of Performance for Electric Utility Steam Generating Units*; US EPA: Washington, DC, USA, 2006.
11. EU. *On the Limitations of Certain Pollutants into the Air from Large Combustion Plants, Directive 2001 /80 /EC of the European Pallament and of Council*; European Union: Brussels, Belgium, 2001.
12. *GB 13223-2011*; Emission Standard of air Pollutants for Thermal Power Plants. Ministry of Ecology and Environment, The People's Republic of China: Beijing, China, 2012.
13. National Development and Reform Commission; Ministry of Environmental Protection; National Energy Administration. Coal Power Energy Saving and Emission Reduction Upgrading and Transformation Action Plan (2014–2020): Development and Transformation Energy [2014] No. 2093 [A/OL]. 12 September 2014. Available online: https://www.ndrc.gov.cn/xxgk/zcfb/tz/201409/t20140919_964234.html?code=&state=123 (accessed on 23 March 2022).
14. Fujian Provincial Environmental Protection Department; Fujian Provincial Economic and Information Technology Commission; Fujian Provincial Development and Reform Commission; Fujian Provincial Price Bureau; Fujian Provincial Energy Regulatory Office. Notice on Printing and Distributing the Work Plan for Comprehensively Implementing Ultra-Low Emission and Energy Conservation Renovation of Coal-fired Power Plants in Fujian Province: Fujian Huanfa [2016] No.6 [A/OL]. 30 January 2016. Available online: http://sthjt.fujian.gov.cn/zwgk/zfxxgkzl/zfxxgkml/mlqtxx/201603/t20160331_107219.htm (accessed on 23 March 2022).
15. Daood, S.; Javed, M.; Gibbs, B.M.; Nimmo, W. NOx control in coal combustion by combining biomass co-firing, oxygen enrich-ment and SNCR. *Fuel* **2013**, *105*, 283–292. [CrossRef]
16. Du, H. Study on Energy Efficiency Evaluation of Layer Combustion Boiler Coupled with Pollutant Emission Reduction and Waste Heat Utilization. Ph.D. Thesis, Harbin Institute of Technology, Harbin, China, 2021. [CrossRef]
17. Jie, Y.; Xin, G.; Yang, L. Application of Low NOx CombustionTechnology in Ultra Low Emission Retrofit of CFB Boilers. *Power Syst. Eng.* **2020**, *36*, 71–72.
18. *DL/T 260-2012*; Electric Power Industry Standard of the People's Republic of China: Code for Performance Acceptance Test of Flue Gas Denitration Device in Coal-Fired Power Plant. State Power Environmental Protection Research Institute: Nanjing, China, 2012.
19. Basu, P. *Circulating Fluidized Bed Boilers: Design Operation and Maintenance*; Springer: Berlin/Heidelberg, Germany, 2015. [CrossRef]
20. Feng, B.; Yuan, J.; Liu, H.; Bo, F.; Jianwei, Y.; Hao, L.; Jianxin, L.; Zhijie, L.; Dechang, L. Study on nitrogen oxide Emission in circulating fluidized bed coal Combustion. *J. Eng. Thermophys.* **1996**, *17*, 125–128.
21. He, H. Experimental and Theoretical Study on the Cleaning Combustion of Fujian Anthracite in CFB Boiler. Ph.D. Thesis, Zhejiang University, Hangzhou, China, 2005.